

# Photolysis of acetophenone derivatives with $\alpha$ -cyclopropyl substituents

Ranaweera A. A. Upul Ranaweera<sup>a</sup>, Geethika K. Weragoda<sup>a</sup>, John Bain<sup>a</sup>, Shinji Watanabe<sup>b</sup>, Manabu Abe<sup>b</sup> and Anna D. Gudmundsdottir<sup>a\*</sup>

Laser flash photolysis of cyclopropyl(phenyl)methanone **6** in argon-saturated methanol yields the triplet ketone ( $T_{1K}$ ) of **6** that is formed with a rate constant of  $\sim 1.7 \times 10^7 \text{ s}^{-1}$  ( $\lambda_{\text{max}} = 360 \text{ nm}$ ) and has a lifetime of  $\sim 1.4 \mu\text{s}$ .  $T_{1K}$  of **6** decays to form ketyl radical **7** ( $\lambda_{\text{max}} \sim 300 \text{ nm}$ ), which dimerizes to form photoproducts, pinacol derivatives **8** and **9**. In comparison, photolysis of *trans*-phenyl(2-phenylcyclopropyl)methanone **1** in argon-saturated chloroform-*d* results in *cis*-phenyl(2-phenylcyclopropyl)methanone **2** and a smaller amount of **3**, presumably through 1,3-biradical **11**. Nanosecond laser flash photolysis of **1** does not reveal significant transient absorption, although the  $T_{1K}$  of **1** is detected with phosphorescence at 77 K. Density functional theory calculations were used to elucidate the triplet reactivity of **1**, **2** and **6** by comparing the feasibility of H atom abstraction, cyclopropyl cleavage and  $\beta$ -quenching of their triplet ketones. Copyright © 2014 John Wiley & Sons, Ltd.

**Keywords:** laser flash photolysis; DFT calculations

## INTRODUCTION

Triplet biradicals have the potential to serve as synthetic precursors for cyclic compounds; biradicals have been used in many synthetic applications to selectively form new carbon–carbon, carbon–oxygen or carbon–nitrogen bonds (Scheme 1).<sup>[1–4]</sup> However, there are several limitations on the use of triplet biradicals for bond formation, such as selective biradical formation and control of intersystem crossing to yield selective product formation. It has been theorized that intersystem crossing in short-chained biradicals, such as 1,2-, 1,3- and 1,4-biradicals, is facilitated by spin–orbit coupling.<sup>[5–9]</sup> In addition, the energy gap between the triplet and singlet surfaces affects intersystem crossing and becomes more efficient as the gap decreases. Because the energy gap and spin–orbit coupling are affected by biradical conformation, control of the reactivity of flexible biradicals is difficult.

Zimmerman *et al.* have shown that photolysis of  $\beta$ -phenyl propiophenone derivative **1** results in the formation of **2** and **3**, and the authors proposed that the formation of **2** and **3** takes place through a 1,3-biradical that also regenerates **1** (Scheme 2).<sup>[1]</sup> More recently, Caldwell *et al.* demonstrated that photolysis of **4** results in **5**.<sup>[10]</sup> By using transient spectroscopy, the authors identified that the isomerization of **4** to **5** takes place through a 1,3-biradical that has a lifetime of  $\sim 13 \text{ ns}$  in methanol.

Interestingly, the ketone chromophores in **1** and **2** have a  $\beta$ -phenyl group; the triplet excited state of  $\beta$ -phenyl aryl ketones with ( $n, \pi^*$ ) configuration are generally unusually short-lived because they are efficiently quenched by an intramolecular process.<sup>[11–20]</sup> The mechanism for  $\beta$ -quenching, however, has not been fully elucidated until recently.<sup>[21,22]</sup> Bucher has proposed that the intramolecular quenching of these  $\beta$ -phenyl aryl ketones takes place through addition of the carboxyl oxygen to the ipso carbon atom in the  $\beta$ -phenyl ring to form a triplet biradical that intersystem crosses to reform the starting material

(Scheme 3).<sup>[23]</sup> This hypothesis was elegantly supported by theoretical calculations<sup>[23]</sup> and reinforced experimentally by investigating  $\beta$ -quenching in 9-phenylphenalenone derivatives.<sup>[21,22]</sup>

We have studied the photochemistry of cyclopropyl derivatives **1** and **6** that have a built-in triplet sensitizer, via product studies, density functional theory (DFT) calculations and nanosecond transient spectroscopy to better understand how cyclopropyl substituents affect the reactivity.

## RESULTS AND DISCUSSION

### Product studies

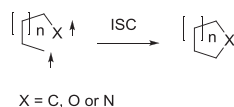
Photolysis of **6** in argon- and oxygen-saturated methanol-*d*<sub>4</sub> through a Pyrex filter ( $>300 \text{ nm}$ ) resulted in dimers **8** and **9**, presumably by the  $T_{1K}$  of **6** abstracting a H atom from the solvent to form ketyl radical **7** (Scheme 4). Thus, ketyl radical **7** must not react with the solvent but instead dimerize in methanol. Furthermore, we did not observe any products from **6** that can be attributed to cleavage of the cyclopropyl ring in ketyl radical **7**. Photolysis of **6** in argon-saturated chloroform-*d* did not yield any photoproducts.

In comparison, photolysis of **1** in argon-saturated chloroform-*d* through a Pyrex filter at ambient temperature yields mainly **2**, a trace amount of **3** and acetophenone (Scheme 5). These

\* Correspondence to: Anna Gudmundsdottir, Department of Chemistry, University of Cincinnati, PO Box 210172, Cincinnati, OH 45221-0172, USA. E-mail: Anna.Gudmundsdottir@uc.edu

a R. A. A. U. Ranaweera, G. K. Weragoda, J. Bain, A. D. Gudmundsdottir  
Department of Chemistry, University of Cincinnati, Cincinnati, OH, 45221-0172, USA

b S. Watanabe, M. Abe  
Department of Chemistry, Graduate School of Science, Hiroshima University, 1-3-1 Kagamiyama, Higashi-Hiroshima, Hiroshima, 739-8526, Japan

**Scheme 1.** Cyclization of biradicals

product studies are in agreement with the earlier reports of Zimmerman *et al.* that photolysis of **1** yields mainly **2** and a small amount of **3**.<sup>[1]</sup> In addition, Zimmerman *et al.* showed that the reaction is reversible; irradiation of **2** results in formation of **1**. We attempted to trap the radicals formed upon photolysis of **1** with oxygen by photolyzing **1** in oxygen-saturated chloroform but obtained only a small amount of benzoic acid as the sole additional product. On the basis of these product studies and the fact that we are irradiating above 300 nm where the ketone chromophores in **1**, **2** and **6** mainly absorb, we propose that the mechanism for the *cis*–*trans* isomerization of both **1** and **2** is as follows: upon irradiation, the ketone absorbs light to form its singlet excited state that intersystem crosses to its triplet configuration (Scheme 5). The triplet ketone reacts to form a 1,3-biradical. Interestingly,  $\beta$ -quenching of the triplet excited state of **2** does not limit its reactivity. In comparison, the triplet ketone in **6** must decay by intermolecular H atom abstraction (Scheme 4). However, product studies are not sufficient to rule out formation of a 1,3-biradical from cleaving the cyclopropyl ring in **6**, as the 1,3-biradical is expected to regenerate **6**.

## Calculations

To compare the reactivities of **1**, **2** and **6** and identify the reason for their different reactivities, we calculated stationary points on their singlet and triplet surfaces using Gaussian09<sup>[24]</sup> at the B3LYP level of theory and with the 6-31+G(d) basis set.<sup>[25,26]</sup>

We optimized the ground-state ( $S_0$ ) of **6** (Fig. 1). The calculations show that the carbonyl group is not fully conjugated with the phenyl group because of steric demands of the cyclopropyl substituent; the torsion angle between C=O and the phenyl group is 10°. Time-dependent DFT (TD-DFT) calculations place the first excited state of the ketone ( $S_{1K}$ ) of **6** at 88 kcal mol<sup>-1</sup>

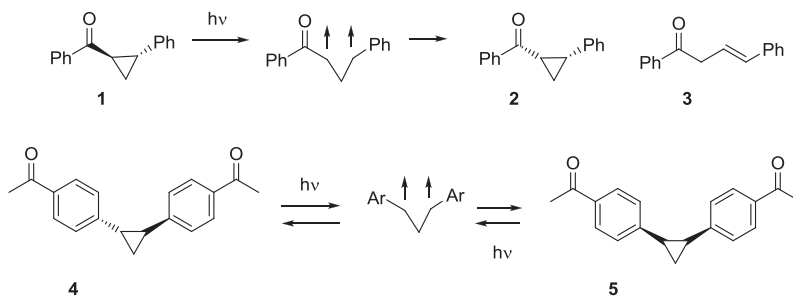
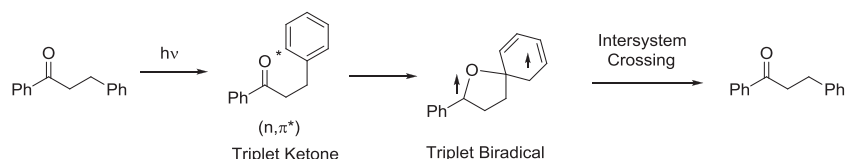
above its ground state ( $S_0$ ) and the first and second triplet excited states ( $T_{1K}$  and  $T_{2K}$ ) of **6** at 76 and 78 kcal mol<sup>-1</sup>, respectively (Fig. 1).

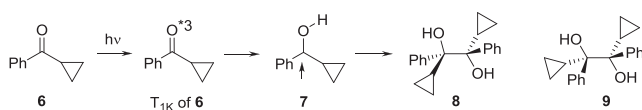
Optimization of the  $T_{1K}$  of **6** reveals that it is 71 kcal mol<sup>-1</sup> above the  $S_0$  of **6**, which is somewhat lower than the energy obtained from TD-DFT calculations (Figs 1 and 2). However, B3LYP calculations generally underestimate the energies of triplet ketones with ( $n, \pi^*$ ) configuration.<sup>[27]</sup> Analysis of the optimized structure of  $T_{1K}$  of **6** shows that the calculated C=O bond is elongated to 1.33 Å, in comparison to 1.22 Å in its  $S_0$ , thus indicating that the  $T_{1K}$  of **6** has ( $n, \pi^*$ ) configuration.<sup>[28]</sup> This result is further supported by spin density calculations that show that the unpaired electron density is mainly located on the carbonyl oxygen and the phenyl moiety (Fig. 1). The calculated torsion angle between the C=O and the phenyl group is increased to 13° in the  $T_{1K}$  of **6** compared with 10° in its  $S_0$  because the C=O bond is longer and therefore needs to rotate away from the cyclopropyl group.

Optimization of 1,3-biradical **10** places it at 51 kcal mol<sup>-1</sup> above the  $S_0$  of **6** (Figs 1 and 2). The C=O and aromatic C–C bonds in **10** are comparable to those in the  $S_0$  of **6** (Fig. 1), whereas the C(O)–C $_{\alpha}$  bond in **10** is calculated to be 1.44 Å and therefore somewhat shorter than the corresponding bond in the  $S_0$  of **6** (1.49 Å). Therefore, the radical on the  $\alpha$ -carbon is conjugated with the C=O moiety, as further supported by spin density calculations that show that the radical centered on the  $\alpha$ -C atom has a spin density of –0.76 and the O atom –0.28. In comparison, the spin density on the  $\gamma$ -carbon atom is –1.02, demonstrating that this second radical is localized on the  $\gamma$ -C atom. Optimization of the singlet configuration of biradical **10** was possible by restricting its  $C_s$  symmetry, showing that it was isoenergetic to its triplet.

The optimization of ketyl radical **7** and CH<sub>2</sub>OH radical places them 67 kcal mol<sup>-1</sup> above the  $S_0$  of **6** and methanol. Calculations show that the spin density in **7** is delocalized over the adjacent phenyl ring and the C atom in the benzylic position (Fig. 1).

The transition state for the  $T_{1K}$  of **6** to form **10** is located 11 kcal mol<sup>-1</sup> above the  $T_{1K}$  of **6**. In comparison, the transition state for the  $T_{1K}$  of **6** to form ketyl radical **7** by H-abstraction from

**Scheme 2.** Isomerization through 1,3-biradicals**Scheme 3.** Proposed mechanism for  $\beta$ -quenching in aryl ketones<sup>[23]</sup>



**Scheme 4.** Proposed mechanism for product formation for **6**

methanol is located  $4 \text{ kcal mol}^{-1}$  above the  $T_{1K}$  of **6** (Fig. 2) and methanol. Comparison of intermolecular reactions with intramolecular rearrangements is generally complicated; however, because methanol is also the solvent for the H atom abstraction, the reaction is pseudo first order and therefore the comparison reasonable. Thus, the calculations support that H atom abstraction should be strongly favored over cleavage of the cyclopropyl ring.

We optimized the  $S_0$  of **1** (Fig. 3); TD-DFT calculations place its  $S_{1K}$  at  $86 \text{ kcal mol}^{-1}$  above its  $S_0$ , whereas the  $T_{1K}$  and  $T_{2K}$  of **1** are  $75$  and  $78 \text{ kcal mol}^{-1}$ , respectively, above its  $S_0$  (Fig. 4). The  $\beta$ -phenyl group is not in close proximity to the carbonyl group; therefore,  $\beta$ -quenching is not important for **1**. However, the carbonyl group is not fully conjugated with the phenyl group, as the torsional angle between C=O and the phenyl group is  $14^\circ$  because of steric demands of the cyclopropyl group.

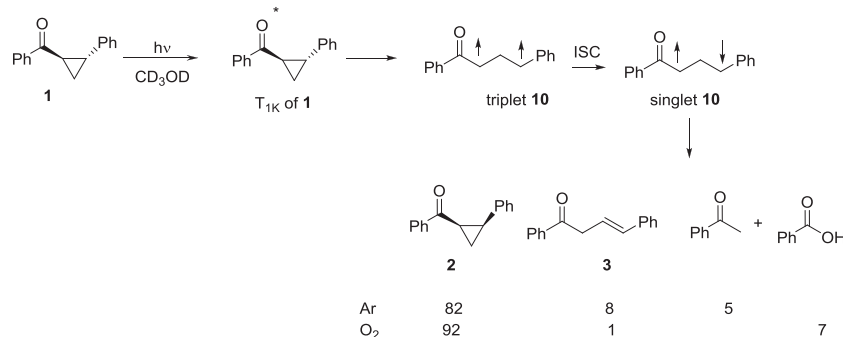
The optimized structure of  $T_{1K}$  of **1** is  $70 \text{ kcal mol}^{-1}$  above the  $S_0$  of **1** (Figs 4 and 5), which is a slightly lower energy than that obtained from TD-DFT calculations. Comparison of the calculated bond lengths in  $T_{1K}$  of **1** to its  $S_0$  shows that the C=O bond elongates in the  $T_{1K}$  of **1** ( $1.32 \text{ \AA}$ ) relative to that in the  $S_0$  of **1** ( $1.22 \text{ \AA}$ ), thus indicating that the  $T_{1K}$  of **1** has ( $n, \pi^*$ )

configuration. This conclusion is further supported by spin density calculations that show that the spin density is mainly located on the carbonyl oxygen and phenyl ring (Fig. 4). The calculations show that the torsion angle between C=O and the phenyl group is reduced to  $5^\circ$  in the  $T_{1K}$  of **1** compared with its  $S_0$ .

Optimization of triplet 1,3-biradical **11** places it  $39 \text{ kcal mol}^{-1}$  above the  $S_0$  of **1**. Both C=O and the aromatic carbon-carbon bonds are similar to the corresponding bonds in the  $S_0$  of **1**, whereas the carbon-carbon bond between C(O)-C and C-Ph are slightly elongated compared with those in the  $S_0$  of **1** because these radical centers are in conjugation with C=O and the phenyl groups. Spin density calculations further support this conclusion (Fig. 4). In addition, as both radical centers in **11** are stabilized by conjugations, the species is more stable relative to its precursor  $T_{1K}$  of **1** than radical **8** to its precursor  $T_{1K}$  of **6**. Because of the conjugation of the C=O group with the  $\alpha$ -C radical, the torsion angle between C=O and the phenyl ring increases to  $14^\circ$ , compared with  $5^\circ$  in the  $T_{1K}$  of **1**. The optimized structure of the singlet configuration of biradical **11** was obtained by restricting its  $C_s$  symmetry and was found to be isoenergetic to its triplet.

Optimization of ketyl radical **12** and  $\cdot\text{CH}_2\text{OH}$  radical places them  $66 \text{ kcal mol}^{-1}$  above  $S_0$  of **1** and methanol (Fig. 5). Spin density calculations show that ketyl radical **12** is delocalized over the phenyl ring, similar to that observed for ketyl radical **7** (Fig. 4).

The calculated transition state for the  $T_{1K}$  of **1** abstracting a H atom from methanol is  $7 \text{ kcal mol}^{-1}$  above the  $T_{1K}$  of **1** (Fig. 5),



**Scheme 5.** Product formation from photolysis of **1**

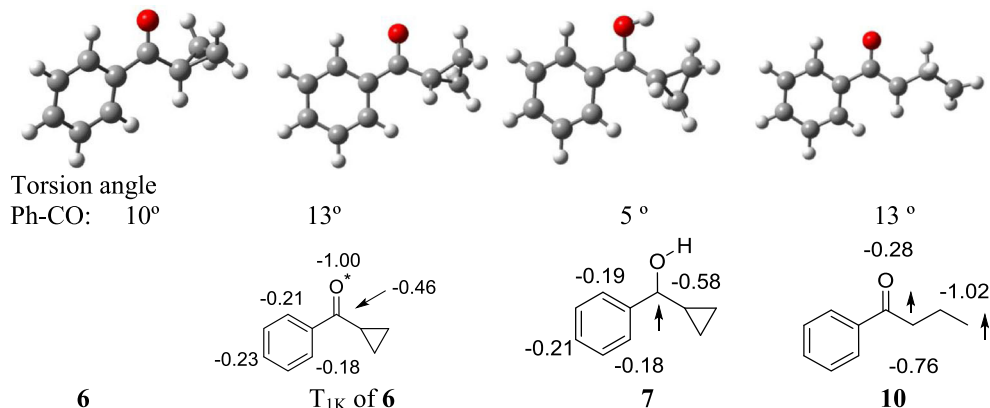


**Figure 1.** Optimized structure of **6**,  $T_{1K}$  of **6**, **7**, **10** and their calculated spin densities

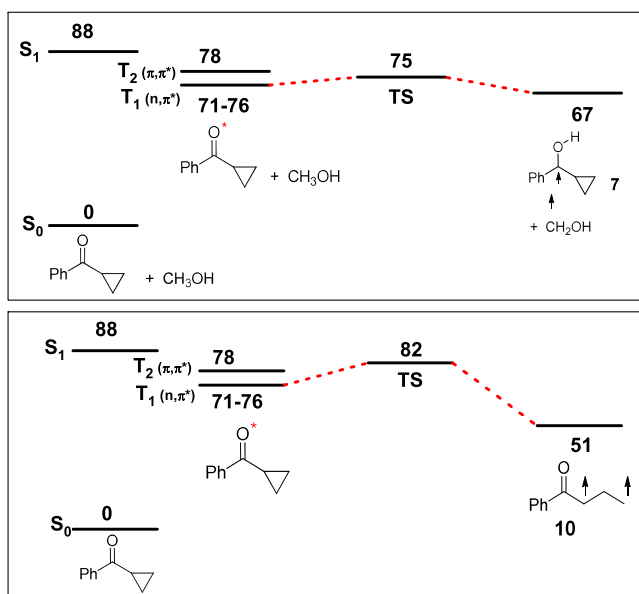


**Figure 2.** Stationary points on the triplet surface of **6**. All energies were obtained with B3LYP/6-31G+(d) optimization, except for the energies for  $S_{1K}$ ,  $T_{2K}$  and  $T_{1K}$  (76) of **6**, which were obtained with TD-DFT calculations (energies are in kcal mol<sup>-1</sup>)

whereas the transition state for the  $T_{1K}$  of **1** to cleave and form the triplet biradical **11** is only 3 kcal mol<sup>-1</sup> above the  $T_{1K}$  of **1**. Thus, the calculations support that the reactivity of  $T_{1K}$  of **1** should strongly favor cleavage of the cyclopropyl ring over H atom abstraction.

The optimized structure of the  $S_0$  of **2** shows that the  $\beta$ -phenyl group is in close proximity to the ketone chromophore; thus,  $\beta$ -quenching is possible (Fig. 6). As for **1**, the calculations show that C=O and the phenyl group are not fully conjugated, as they have a torsional angle of 14°. TD-DFT calculations place the  $S_1$  of **2** at 86 kcal mol<sup>-1</sup> and the  $T_1$  and  $T_2$  at 75 and 78 kcal mol<sup>-1</sup>, respectively, above their  $S_0$ , which is similar as those calculated for **1** (Fig. 7).

Optimization of the  $T_{1K}$  of **2** places it 69 kcal mol<sup>-1</sup> above its  $S_0$ , which is, as expected, somewhat lower than the energy

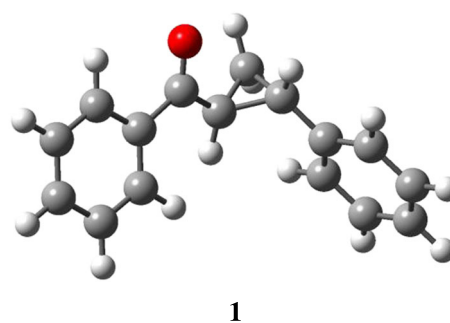


**Figure 3.** Optimized  $S_0$  structure of **1**. The calculated CO-Ph torsional angle is 14°

obtained from TD-DFT calculations. The calculated C=O bond of  $T_{1K}$  of **2** is prolonged to 1.32 Å, which, along with the spin density calculations, suggests that the  $T_{1K}$  of **2** has a (n,  $\pi^*$ ) configuration. The  $\beta$ -phenyl group is in close approximation to the carbonyl group, as the calculated distances between the oxygen and ipso carbon atoms are 2.88 and 3.77 Å. Furthermore, the calculated torsional angle between C=O and the phenyl group in the  $T_{1K}$  of **2** is similar to that in its  $S_0$ ; the steric demand of the substituted cyclopropyl group is larger than for the  $T_{1K}$  of **1**.

The optimized structure of **13** places it 65 kcal mol<sup>-1</sup> above the  $S_0$  of **2** (Fig. 7). Spin density calculations show that the spin density is mainly localized on the  $\beta$ -phenyl group and the carbonyl carbon atom adjacent to the  $\alpha$ -phenyl group.

Finally, we calculated the transition state barriers for the  $T_{1K}$  of **2** forming biradical **13** and abstracting a H atom from methanol (Fig. 7). These barriers are very similar to those obtained for the  $T_{1K}$  of **1** (Fig. 5). Interestingly, the calculated transition barrier for the addition of an oxygen atom to the ipso carbon atom is comparable with the transition state barrier for formation of triplet biradical **11**. Thus, the calculations support that formation of biradical **11** from the  $T_{1K}$  of **2** can compete with  $\beta$ -quenching.

The calculations suggest that H atom abstraction should be strongly favored for the  $T_{1K}$  of **6** over cleavage to form 1,3-biradical **10**. Similarly, the calculations suggest that the  $T_{1K}$  of **1** and the  $T_{1K}$  of **2** undergo cleavage of the cyclopropyl ring to form biradical **11** rather than H atom abstraction. In addition,

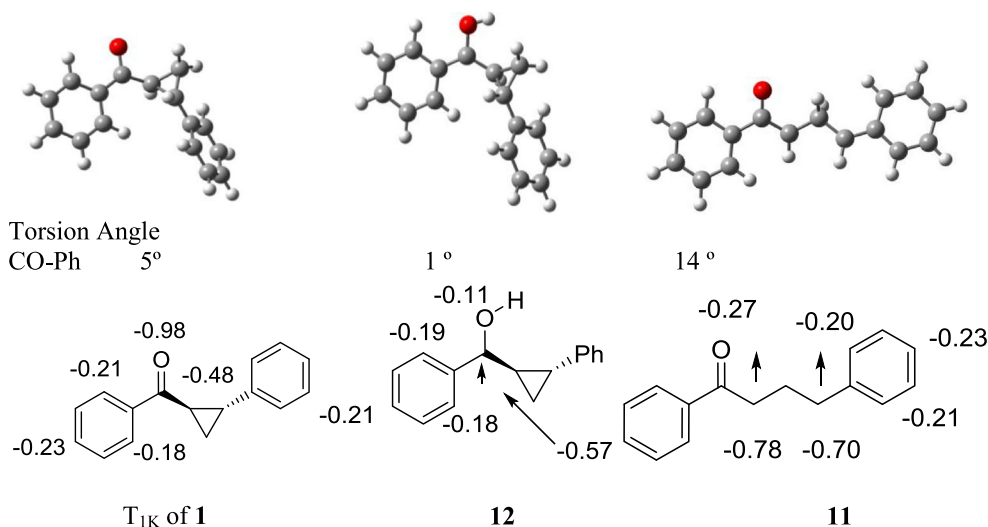


**Figure 4.** Optimized structures of the  $T_{1K}$  of **1**, ketyl radical **12** and biradical **11** and their spin densities

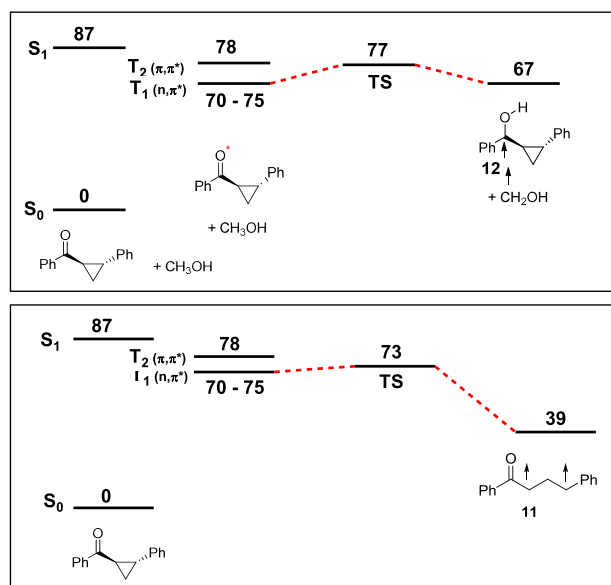


**Figure 5.** Stationary points on the triplet surface of **1**. All calculations were obtained by optimization with B3LYP/6-31G+(d), except for the energies of the  $S_{1K}$ ,  $T_{2K}$  and  $T_{1K}$  (**75**) of **1**, which were obtained with TD-DFT/B3LYP/6-31G+(d) calculations (energies are in  $\text{kcal mol}^{-1}$ )

the calculations show that there is a significant steric effect of the cyclopropyl substituents in the  $S_0$  and  $T_{1K}$  of **1**, **2** and **6** that decreases the conjugation between  $\text{C}=\text{O}$  and the  $\alpha$ -phenyl groups. Furthermore, the calculations demonstrate that the transition state barriers for the  $T_{1K}$  of **2**  $\beta$ -quenching and formation of biradical **11** are comparable.

### Phosphorescence

The phosphorescence spectrum of **6** is displayed in Fig. 8. The (0, 0) transition is located at 385 nm, which corresponds to the  $T_{1K}$  of **6** with energy of  $74 \text{ kcal mol}^{-1}$ , in excellent agreement with the value obtained from a TD-DFT calculation ( $76 \text{ kcal mol}^{-1}$ ). The phosphorescence spectrum of **1** has the (0, 0) transition at 396 nm (Fig. 8), which corresponds to

$72 \text{ kcal mol}^{-1}$ , also in good agreement with the calculated value of  $75 \text{ kcal mol}^{-1}$ . The phosphorescence obtained for **1** and **6** demonstrates that, upon irradiation, their triplet ketones are populated.

### Laser flash photolysis

We used laser flash photolysis to identify the intermediates formed upon photolysis of **1** and **6**. Laser flash photolysis (Excimer laser, 308 nm)<sup>[29]</sup> of **6** in argon-saturated methanol produced a transient absorption with  $\lambda_{\text{max}}$  at  $\sim 360 \text{ nm}$  (Fig. 9). We assign this absorption at 360 nm to the  $T_{1K}$  of **6** and ketyl radical **7** based on calculations. The calculated TD-DFT spectrum of the  $T_{1K}$  of **6** in methanol has major electronic transfer at 383 ( $f=0.0596$ ), 305 ( $f=0.0232$ ) and 303 nm ( $f=0.0418$ ; Fig. 10), which fits well with the observed spectrum. TD-DFT calculations of ketyl radical **7** in methanol place the major electron transitions at 377 ( $f=0.0193$ ) and 315 nm ( $f=0.0302$ ; Fig. 10), which is somewhat similar to the observed spectra of the  $T_{1K}$  of **6** with less intensive electronic transitions.

Kinetic analysis of the transient absorption at 360 nm shows that, in argon-saturated methanol, transient absorption is formed with a rate constant of  $1.7 \times 10^7 \text{ s}^{-1}$  ( $\tau \sim 60 \text{ ns}$ ) and decays with a rate constant of  $7.1 \times 10^5 \text{ s}^{-1}$  ( $\sim 1.4 \mu\text{s}$ ; Fig. 11). In oxygen-saturated methanol, the absorption at 360 nm is fully quenched. We assign the transient to the  $T_{1K}$  of **6**. Quenching studies with isoprene further support this assignment, as the absorption at 360 nm decayed faster as the concentration of isoprene increased. The observed rate constant for the decay of  $T_{1K}$  of **6** is displayed in Fig. 12 as a function of isoprene concentration, and the quenching rate of  $T_{1K}$  of **6** with isoprene is  $8.3 \times 10^9 \text{ M}^{-1} \text{ s}^{-1}$ .

At 320 nm, the absorption is formed with the same rate constant as at 360 nm. In addition, the absorption at 320 nm shows a fast decay that can be fitted to the same rate constant as the decay at 360 nm and is significantly slower decay than that assigned to ketyl radical **7**. Because there is also significant residual absorption due to product formation at 320 nm, precise estimation of the lifetime of ketyl radical **7** is complicated.

Laser flash photolysis (Excimer laser, 308 nm) of **1** in argon-saturated methanol and chloroform shows a depletion of the

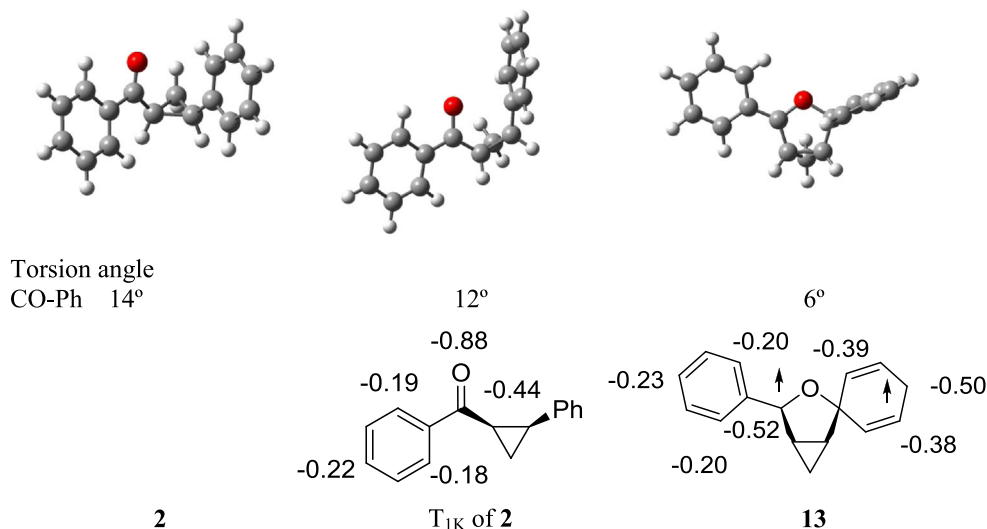


**Figure 6.** Optimized structures of **2**,  $T_{1K}$  of **2** and biradical **13** and their calculated spin densities

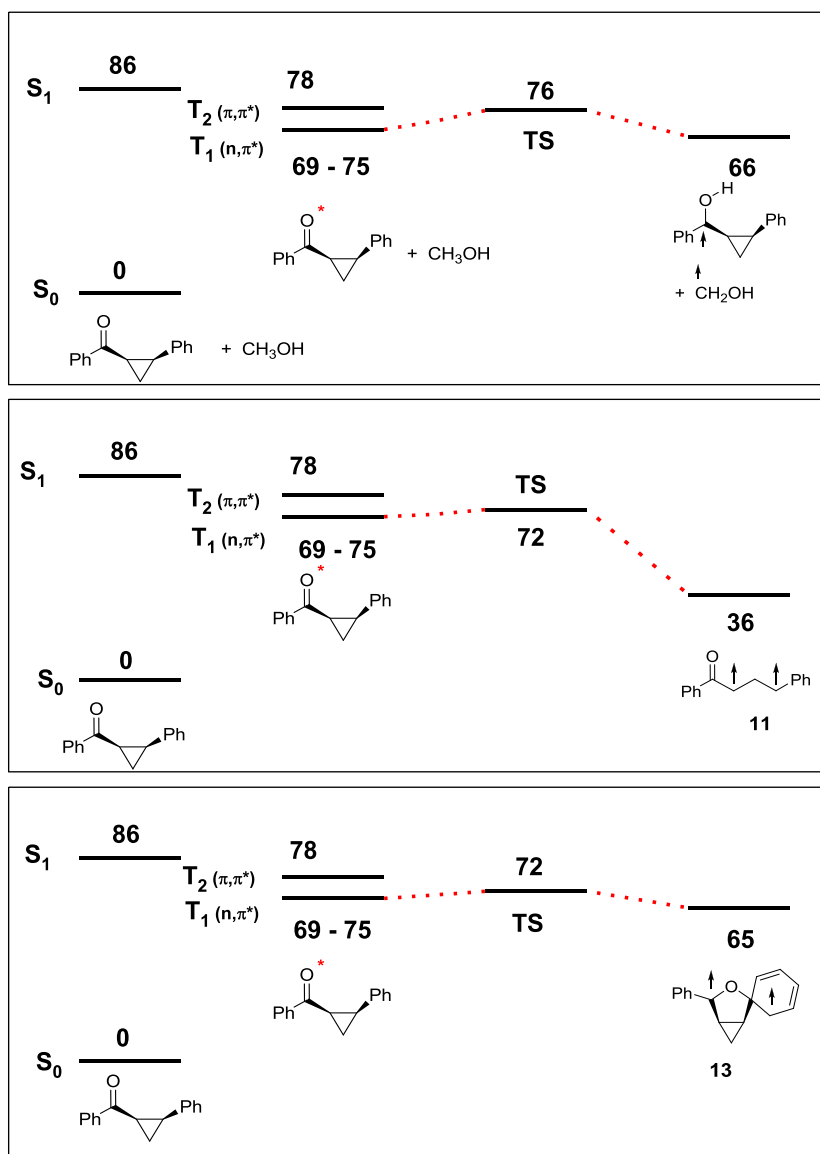


**Figure 7.** Stationary points on the triplet surface of **2**. All energies were obtained by optimization with B3LYP/6-31G+(d), except for the energies of the  $S_{1K}$ ,  $T_{2K}$  and  $T_{1K}$  (**75**) of **2**, which were obtained with time TD-DFT/B3LYP/6-31G+(d) calculations (energies are in kcal mol<sup>-1</sup>)

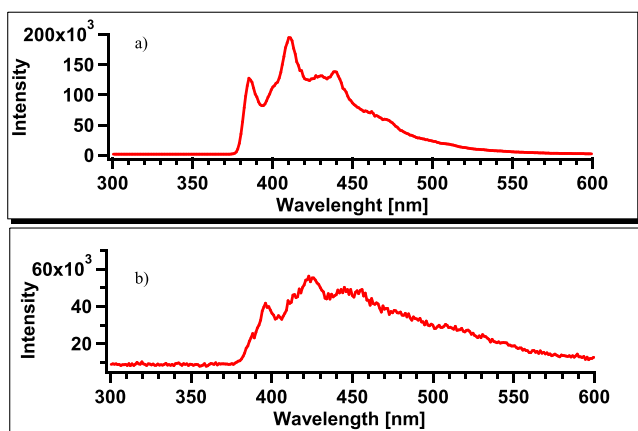


**Figure 8.** Phosphorescence spectra at 77 K of (a) **6** (50 mM) and (b) **1** (5 mM) in ethanol with 300-nm excitation

starting material approximately 340 and 400 nm. We were not able to detect any significant transient absorption due to the  $T_{1K}$  of **1**, which is expected to have  $\lambda_{\max}$  approximately 420 nm based on TD-DFT calculations in methanol (Fig. 13), or triplet biradical **11**, which is expected to have a broad absorption between 300 and 460 nm.

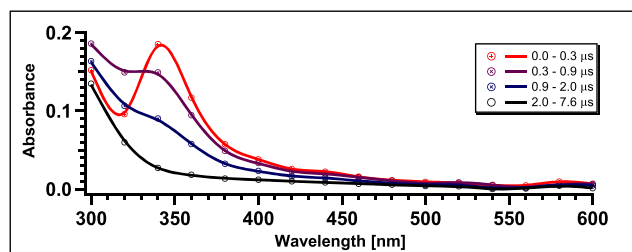


**Figure 9.** Transient spectra obtained by laser flash photolysis of **6** in argon-saturated methanol

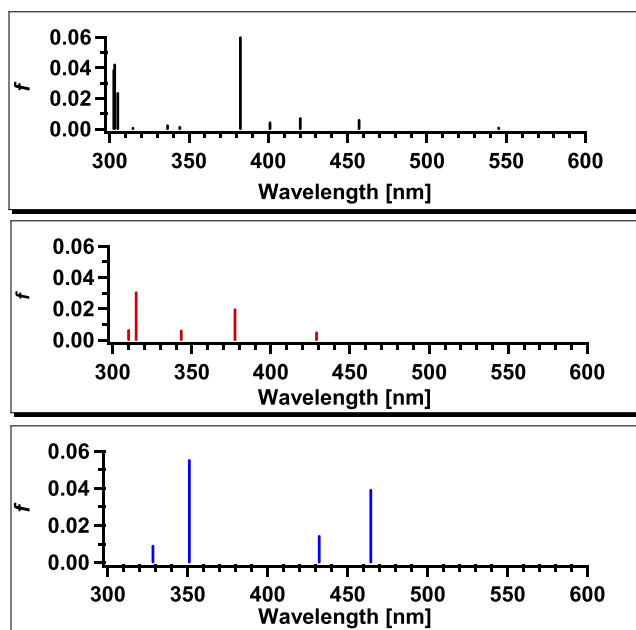


**Figure 10.** Calculated absorption spectra of the  $T_{1K}$  of **6** (black), ketyl radical **7** (red) and triplet biradical **10** (blue) in methanol

### ESR spectroscopy

ESR spectroscopy of **1** at 10 and 80 K in ethanol with 355 nm laser irradiation did not yield an ESR signal, indicating that triplet biradical **10** is short-lived and can decay to its singlet configuration efficiently.

## DISCUSSION

We have shown that irradiation of **6** results in reduction of the ketone through intermolecular H atom abstraction and that the activation barrier for cleavage of the cyclopropyl ring is too large to compete with H atom abstraction. Furthermore, we have verified that the photoreactivity of **6** takes place on its triplet surface, although the rate of intersystem crossing in **6** ( $1.7 \times 10^7 \text{ s}^{-1}$ ) is very slow in comparison to intersystem crossing in acetophenone ( $4 \times 10^{10} \text{ s}^{-1}$ ).<sup>[30]</sup> The rate of intersystem crossing in **6** is more similar to that observed for aliphatic ketones such as acetone ( $5 \times 10^8 \text{ s}^{-1}$ ) or aromatic hydrocarbons

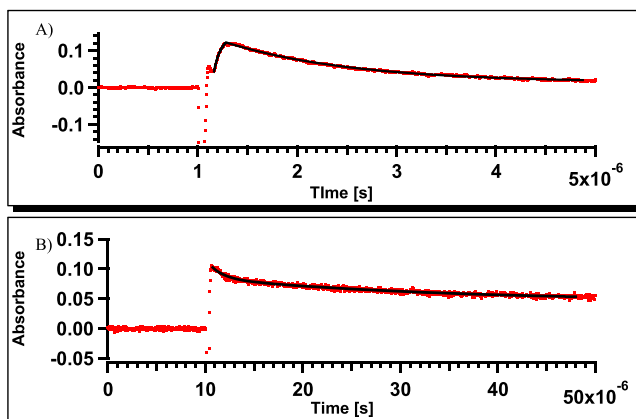


**Figure 11.** Kinetic traces obtained from laser flash photolysis of **6** in argon-saturated methanol at (A) 360 and (B) 320 nm

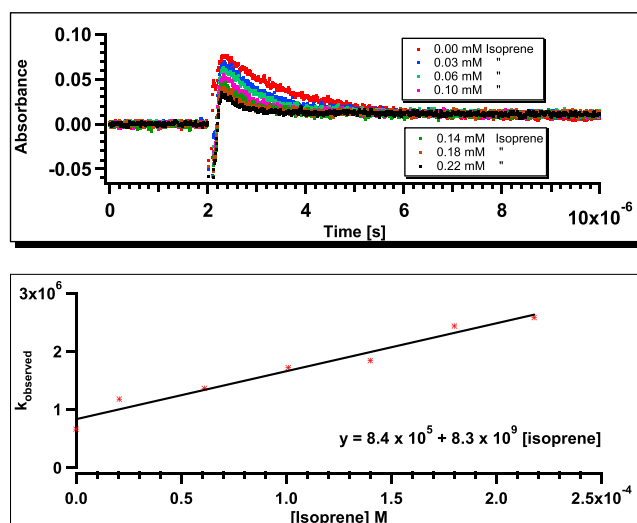


**Figure 12.** Rate constant for the decay at 360 nm as a function of isoprene concentration

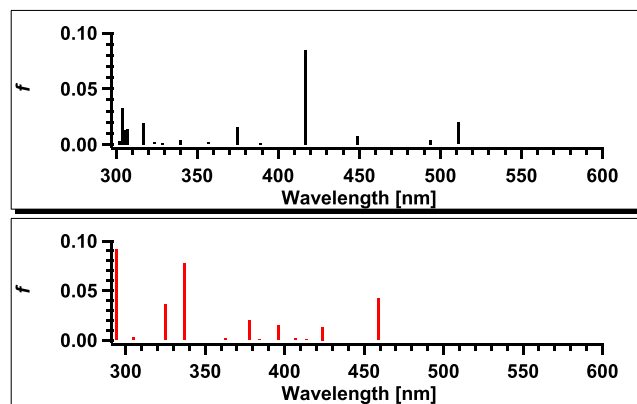
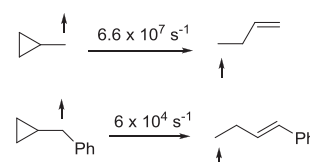


**Figure 13.** Calculated absorption spectra of the  $T_{1K}$  of **1** (black) and **11** (red) in methanol

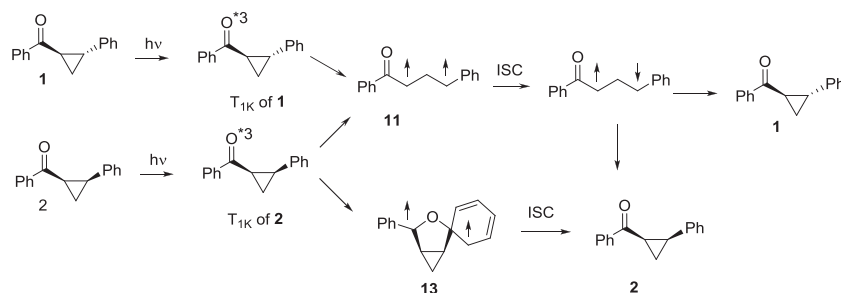
such as triphenylene ( $5 \times 10^7 \text{ s}^{-1}$ ).<sup>[31]</sup> Therefore, the steric demand of the cyclopropyl group in **6** influences the intersystem crossing rate to form the  $T_{1K}$  of **6**.

As noted earlier, no products were observed that can be attributed to ketyl radical **7** undergoing ring opening rearrangement of its cyclopropyl group, and therefore, ketyl radical **7** does not act as a radical clock. This is an agreement with what Newcomb *et al.*<sup>[32,33]</sup> reported that cyclopropylcarbinyl phenyl radical rearranges much slower than cyclopropylcarbinyl radical that has been utilized as radical clock<sup>[34]</sup> (Scheme 6). Thus, it is reasonable that ketyl radical **7** decays by reacting with solvent rather than undergoing ring opening rearrangement of its cyclopropyl moiety.

In comparison, we have shown that ketone **1** does not undergo H atom abstraction, as the calculated transition state



**Scheme 6.** Cyclopropylcarbinyl radical rearrangements



**Scheme 7.** Proposed photoreaction mechanism for **1** and **2**

barrier for H atom abstraction is considerably larger than the barrier for cyclopropyl ring cleaving. We did not observe the  $T_{1K}$  of **1** and **2** or biradical **10** with laser flash photolysis or ESR spectroscopy. However, the detection of the phosphorescence of the  $T_{1K}$  of **1** verifies that the photoreactivity of **1** takes place on its triplet surface, just as is observed for **6**. Thus, we expect the  $T_{1K}$  of **1** to be formed at a similar rate as the  $T_{1K}$  of **6** and to decay to form triplet biradical **11**. Because the triplet and singlet configurations of biradical **11** are isoenergetic, intersystem crossing from triplet to singlet must be very efficient, which explains the short lifetime of biradical **11** that cannot be detected with a nanosecond laser flash photolysis apparatus (17 ns time resolution). Biradical **11** must be somewhat shorter lived than similar biradicals observed by Caldwell *et al.*, which had lifetimes of a few nanoseconds.<sup>[35]</sup> The biradical formed from photolysis of **4** and **5** is longer lived than biradical **11**, presumably allowing it, but not biradical **11**, to be successfully trapped with oxygen. Furthermore, the rate constant for forming  $T_{1K}$  of **1** is expected to be similar to that observed for the  $T_{1K}$  of **6**, and the calculated transition state barrier for transformation of the  $T_{1K}$  of **1** to biradical **11** is lower than that for H atom abstraction of the  $T_{1K}$  of **6**; therefore, the lifetime of the  $T_{1K}$  of **1** should be less than that of the  $T_{1K}$  of **6**. The rate constants for the decay of the  $T_{1K}$  of **1** and biradical **11** are likely less than the rate constant for intersystem crossing to form the  $T_{1K}$  of **1**; thus, we do not observe the  $T_{1K}$  of **1** or biradical **11** at ambient temperature with laser flash photolysis.

Interestingly, although the carbonyl group in the  $T_{1K}$  of **2** is perfectly aligned for  $\beta$ -quenching,  $\beta$ -quenching does not limit the reactivity of **2** because the transition state barriers for  $\beta$ -quenching and formation of 1,3-biradical are similar.  $\beta$ -Quenching is not efficient enough to restrict cleavage of the cyclopropyl of **2**; thus, photolysis cannot be used to selectively form **2** from **1**. The proposed reaction mechanism for the *cis-trans* isomerization of **1** and **2** also takes into account the  $\beta$ -quenching of the  $T_{1K}$  of **2**, as shown in Scheme 7.

Although intramolecular sensitization with a built-in triplet acetophenone sensitizer has been shown to be a valuable tool for forming triplet biradicals such as triplet alkylnitrenes and vinylnitrenes,<sup>[36–42]</sup> intramolecular sensitization using acetophenone derivatives with  $\alpha$ -cyclopropyl substituents is complicated by slow intersystem crossing rates.

## CONCLUSION

We have shown that intersystem crossing rates in acetophenone derivatives with  $\alpha$ -cyclopropyl substituents are only on the order of  $10^7 \text{ s}^{-1}$  and therefore more similar to intersystem crossing

rates in aromatic hydrocarbons and aliphatic ketones than aryl ketones. Photolysis of **6** in methanol results in H atom abstraction on the triplet surface. As the phosphorescence of the  $T_{1K}$  of **1** is observed at a low temperature, we conclude that **1** reacts on its triplet surface to yield biradical **11**, which intersystem crosses to regenerate **1** and its *cis* isomer **2**. DFT calculations predict that cleavage of **2** to form triplet biradical **11** is comparable with  $\beta$ -quenching or formation of biradical **13**.

## EXPERIMENTAL

### Calculations

All geometries were optimized at the B3LYP level of theory and with the 6-31G+(d) basis set as implemented in the Gaussian09 programs.<sup>[24,25,43]</sup> All transition states were confirmed to have one imaginary vibrational frequency by analytical determination of the second derivatives of energy with respect to internal coordinates. Intrinsic reaction coordinate calculations were used to verify that the located transition states corresponded to the attributed reactant and product.<sup>[44,45]</sup> The absorption spectra were calculated using TD-DFT calculations.<sup>[46–50]</sup> The effect of solvation was calculated using the self-consistent reaction field method with the integral equation formalism polarization continuum model with methanol and dichloromethane as solvents.<sup>[51–55]</sup>

### Laser flash photolysis

Laser flash photolysis was performed with an Excimer laser (308 nm, 17 ns). The system has been described in detail elsewhere.<sup>[56]</sup> A stock solution of **1** and **6** in  $\text{CH}_3\text{OH}$  was prepared with spectroscopic grade  $\text{CH}_3\text{OH}$ , such that the solution had an absorption between 0.3 and 0.6 at 308 nm. Typically,  $\sim 2 \text{ mL}$  of the stock solution was placed in a  $10 \text{ mm} \times 10 \text{ mm}$  wide, 48 mm long quartz cuvette and was purged with argon for 5 min or oxygen for 15 min. The rates were obtained by fitting an average of three to five kinetic traces.

### Phosphorescence

Phosphorescence measurements were carried out at 77 K with 300-nm irradiation.<sup>[6]</sup>

### Electron Spin Resonance spectroscopy

Steady-state ESR measurements were taken at 10 K and at 80 K in ethanol glass in a Bruker ESR E500 spectrometer with an INDI-10 YAG laser source with 355-nm irradiation and 80-mW laser beam.

### Photolysis of **1** and **6**

Compounds **1** and **6** were purchased from Ottawa Chemicals, Ukraine, and Aldrich, USA, respectively. The spectroscopic characterization of **1** and **6** are as follows. **6**:  $^1\text{H}$  NMR ( $\text{CDCl}_3$ , 400 MHz):  $\delta$  1.018–1.064

(m,2H), 1.226–1.264 (m, 2H), 2.649–2.711 (m, 1H), 7.472 (t,  $J=7.2$  Hz, 2H), 7.561 (t,  $J=7.2$  Hz, 1H), 8.018 (d,  $J=7.2$  Hz, 2H) ppm; GC/MS (EI):  $m/z$  146 ( $M^+$ ), 131, 127, 119, 115, 105 (100%), 98, 91, 87, 77, 73, 69, 63, 59, 55, 51.

**1:**  $^1\text{H}$  NMR ( $\text{CDCl}_3$ , 400 MHz):  $\delta$  1.529–1.575 (m, 1H), 1.901–1.946 (m, 1H), 2.674–2.723 (m, 1H), 2.877–2.920 (m, 1H), 7.17 (d,  $J=7.2$  Hz, 2H), 7.22 (t,  $J=7.2$  Hz, 1H), 7.306 (t,  $J=7.2$  Hz, 2H), 7.45 (d,  $J=7.6$  Hz, 2H), 7.548 (t,  $J=7.6$  Hz, 1H), 7.99 (d,  $J=7.6$  Hz, 2H) ppm; GC/MS (EI):  $m/z$  222 ( $M^+$ ), 207, 200, 193, 178, 165, 152, 144, 131, 115, 105 (100%), 97, 91, 85, 77, 63, 57, 51.

### Product studies of **6** in argon-saturated $\text{CD}_3\text{OD}$

A solution of **6** (~50 mg, 0.3 mmol) in  $\text{CD}_3\text{OD}$  (2 mL) was purged with argon and photolyzed via a Pyrex filter for 94 h at 298 K.  $^1\text{H}$  NMR and GC/MS analysis of the reaction mixture showed the formation of **8** and **9** (37%) with some remaining starting material (57%). The products were characterized by GC/MS chromatography of the reaction mixture.

**8** and **9:** GC/MS (EI):  $m/z$  148 ( $M^+/2$ ), 128, 115, 105, 91, 77, 69, 51.

### Product studies of **6** in oxygen-saturated $\text{CH}_3\text{OH}$

A solution of **6** (~50 mg, 0.3 mmol) in  $\text{CH}_3\text{OH}$  (2 mL) was purged with oxygen and photolyzed via a Pyrex filter for 94 h at 298 K.  $^1\text{H}$  NMR and GC/MS analysis of the reaction mixture showed the formation of **8** and **9** (15%) with some remaining starting material (77%). The products were characterized by GC/MS chromatography of the reaction mixture.

### Product studies of **1** in argon-saturated $\text{CDCl}_3$

A solution of **1** (~50 mg, 0.2 mmol) in  $\text{CD}_3\text{OD}$  (2 mL) was purged with argon and photolyzed via a Pyrex filter for 34 h at 298 K.  $^1\text{H}$  NMR and GC/MS analysis of the reaction mixture showed the formation of acetophenone (5%), **2** (82%) and **3** (8%) at 60% conversion. The products were characterized by GC/MS chromatography and  $^1\text{H}$  NMR spectroscopy of the reaction mixture.

**2:**  $^1\text{H}$  NMR ( $\text{CDCl}_3$ , 400 MHz):  $\delta$  1.428–1.480 (m, 1H), 2.092–2.137 (m, 1H), 2.852–2.924 (m, 1H), 3.062–3.132 (m, 1H), 7.090–7.127 (m, 1H), 7.156–7.192 (m, 3H), 7.359–7.510 (m, 4H), 7.901 (d,  $J=8.0$  Hz, 2H) ppm; GC/MS (EI):  $m/z$  222 ( $M^+$ ), 207, 200, 193, 178, 165, 152, 144, 131, 115, 105 (100%), 97, 91, 83, 77, 63, 57, 51.

**3:** GC/MS (EI):  $m/z$  222 ( $M^+$ ), 165, 115, 105 (100%), 91, 77, 63, 51.

### Product studies of **1** in argon-saturated $\text{CD}_3\text{OD}$

A solution of **1** (~50 mg, 0.2 mmol) in  $\text{CD}_3\text{OD}$  (2 mL) was purged with argon and photolyzed via a Pyrex filter for 34 h at 298 K.  $^1\text{H}$  NMR and GC/MS analysis of the reaction mixture showed the formation of **2** (92%) and benzoic acid (8%) at 48% conversion. The products were characterized by GC/MS chromatography and  $^1\text{H}$  NMR spectroscopy of the reaction mixture.

**2:**  $^1\text{H}$  NMR ( $\text{CDCl}_3$ , 400 MHz):  $\delta$  1.428–1.480 (m, 1H), 2.092–2.137 (m, 1H), 2.852–2.924 (m, 1H), 3.062–3.132 (m, 1H), 7.09–7.13 (m, 1H), 7.16–7.19 (m, 3H), 7.36–7.51 (m, 4H), 7.90 (d,  $J=8.0$  Hz, 2H) ppm; GC/MS (EI):  $m/z$  222 ( $M^+$ ), 207, 200, 193, 178, 165, 152, 144, 131, 115, 105 (100%), 97, 91, 83, 77, 63, 57, 51.

**3:** GC/MS (EI):  $m/z$  222 ( $M^+$ ), 165, 115, 105 (100%), 91, 77, 63, 51.

## Acknowledgements

This work was supported by the National Science Foundation and the Ohio Supercomputer Center. R. A. A. U. R. acknowledges the University of Cincinnati Research Council for a URC Fellowship and J. B. NSF-REU for a summer Fellowship. A. D. G. is grateful for the opportunity to spend a sabbatical in the laboratory of Professor Abe as a Fulbright Scholar.

## REFERENCES

- H. E. Zimmerman, R. W. Binkley, *Tetrahedron Lett.* **1985**, 26, 5859.
- S. Z. Zard, *Chem. Soc. Rev.* **2008**, 37, 1603.
- A. Griesbeck, M. Oelgemoller, F. Ghetti, *Editors, CRC Handbook of Organic Photochemistry and Photobiology*, 3rd edn., Volume 1, CRC Press, Boca Raton, FL, **2012**.
- Eds: A. G. Griesbeck, J. Mattay, *Synthetic Organic Photochemistry. [In: Mol. Supramol. Photochem.; 2005, 12]*, Marcel Dekker, Inc., New York, **2005**.
- R. A. Caldwell, *Pure Appl. Chem.* **1984**, 56, 1167.
- R. A. A. U. Ranaweera, T. Scott, Q. Li, S. Rajam, A. Duncan, R. Li, A. Evans, C. Bohne, J. P. Toscano, B. S. Ault, A. D. Gudmundsdottir, *J. Phys. Chem. A* **2014**, ASAP. DOI: 10.1021/jp504174t
- F. Kita, W. M. Nau, W. Adam, J. Wirz, *J. Am. Chem. Soc.* **1995**, 117, 8670.
- A. G. Kutateladze, *J. Am. Chem. Soc.* **2001**, 123, 9279.
- A. G. Griesbeck, M. Abe, S. Bondock, *Acc. Chem. Res.* **2004**, 37, 919.
- N. Ichinose, K. Mizuno, Y. Otsuji, R. A. Caldwell, A. M. Helms, *J. Org. Chem.* **1998**, 63, 3176.
- J. C. Scaiano, M. J. Perkins, J. W. Sheppard, M. S. Platz, R. L. Barcus, *J. Photochem.* **1983**, 21, 137.
- T. Wismontski-Knittel, T. Kilp, *J. Phys. Chem.* **1984**, 88, 110.
- J. C. Netto-Ferreira, W. J. Leigh, J. C. Scaiano, *J. Am. Chem. Soc.* **1985**, 107, 2617.
- R. Boch, C. Bohne, J. C. Netto-Ferreira, J. C. Scaiano, *Can. J. Chem.* **1991**, 69, 2053.
- W. J. J. Leigh, *J. Chem. Soc. Chem. Comm.* **1993**, 988.
- J. N. Moorthy, W. S. Patterson, C. Bohne, *J. Am. Chem. Soc.* **1997**, 119, 11094.
- J. N. Moorthy, S. L. Monahan, R. B. Sunoj, J. Chandrasekhar, C. Bohne, *J. Am. Chem. Soc.* **1999**, 121, 3093.
- S. Samanta, B. K. Mishra, T. C. S. Pace, N. Sathyamurthy, C. Bohne, J. N. Moorthy, *J. Org. Chem.* **2006**, 71, 4453.
- D. Ng, Z. Yang, M. A. Garcia-Garibay, *Tetrahedron Lett.* **2001**, 42, 9113.
- P. J. Wagner, P. A. Kelso, A. E. Kempainen, A. Haug, D. R. Graber, *Mol. Photochem.* **1970**, 2, 81.
- O. Anamimoghadam, M. D. Symes, C. Busche, D.-L. Long, S. T. Caldwell, C. Flors, S. Nonell, L. Cronin, G. Bucher, *Org. Lett.* **2013**, 15, 2970.
- G. Bucher, R. Bresoli-Obach, C. Brosa, C. Flors, J. G. Luis, T. A. Grillo, S. Nonell, *Phys. Chem. Chem. Phys.* **2014**, 16, 18813.
- G. Bucher, *J. Phys. Chem. A* **2008**, 112, 5411.
- M. J. Frisch, G. W. Trucks, H. B. Schlegel, G. E. Scuseria, M. A. Robb, J. R. Cheeseman, G. Scalmani, V. Barone, B. Mennucci, G. A. Petersson, H. Nakatsuji, M. Caricato, X. Li, H. P. Hratchian, A. F. Izmaylov, J. Bloino, G. Zheng, J. L. Sonnenberg, M. Hada, M. Ehara, K. Toyota, R. Fukuda, J. Hasegawa, M. Ishida, T. Nakajima, Y. Honda, O. Kitao, H. Nakai, T. Vreven, J. A. Montgomery, J. E. Peralta, F. Ogliaro, M. Bearpark, J. J. Heyd, E. Brothers, K. N. Kudin, V. N. Staroverov, R. Kobayashi, J. Normand, K. Raghavachari, A. Rendell, J. C. Burant, S. S. Iyengar, J. Tomasi, M. Cossi, N. Rega, J. M. Millam, M. Klene, J. E. Knox, J. B. Cross, V. Bakken, C. Adamo, J. Jaramillo, R. Gomperts, R. E. Stratmann, O. Yazyev, A. J. Austin, R. Cammi, C. Pomelli, J. W. Ochterski, R. L. Martin, K. Morokuma, V. G. Zakrzewski, G. A. Voth, P. Salvador, J. J. Dannenberg, S. Dapprich, A. D. Daniels, Farkas, J. B. Foresman, J. V. Ortiz, J. Cioslowski, D. J. Fox, Wallingford CT, **2009**.
- A. D. Becke, *J. Chem. Phys.* **1993**, 98, 5648.
- C. Lee, W. Yang, R. G. Parr, *Phys. Rev. B* **1988**, 37, 785.
- S. Muthukrishnan, S. M. Mandel, J. C. Hackett, P. N. D. Singh, C. M. Hadad, J. A. Krause, A. D. Gudmundsdottir, *J. Org. Chem.* **2007**, 72, 2757.
- S. Srivastava, E. Yourd, J. P. Toscano, *J. Am. Chem. Soc.* **1998**, 120, 6173.
- S. Muthukrishnan, J. Sankaranarayanan, R. F. Klima, T. C. S. Pace, C. Bohne, A. D. Gudmundsdottir, *Org. Lett.* **2009**, 11, 2345.
- P. F. McGarry, C. E. Doubleday Jr, C.-H. Wu, H. A. Staab, N. J. Turro, *J. Photochem. Photobio. A* **1994**, 77, 109.
- G. V. Büнау, *Ber. Bunsenges. Phys. Chem.* **1970**, 74, 1294.
- M. Newcomb, N. Tanaka, A. Bouvier, C. Tronche, J. H. Horner, O. M. Musa, F. N. Martinez, *J. Am. Chem. Soc.* **1996**, 118, 8505.
- T. A. Halgren, J. D. Roberts, J. H. Horner, F. N. Martinez, C. Tronche, M. Newcomb, *J. Am. Chem. Soc.* **2000**, 122, 2988.
- V. W. Bowry, J. Luszyk, K. U. Ingold, *J. Am. Chem. Soc.* **1991**, 113, 5687.

- [35] R. A. Caldwell, *Pure Appl. Chem.* **1984**, *56*, 1167.
- [36] P. N. D. Singh, S. M. Mandel, R. M. Robinson, Z. Zhu, R. Franz, B. S. Ault, A. D. Gudmundsdóttir, *J. Org. Chem.* **2003**, *68*, 7951.
- [37] P. N. D. Singh, S. M. Mandel, J. Sankaranarayanan, S. Muthukrishnan, M. Chang, R. M. Robinson, P. M. Lahti, B. S. Ault, A. D. Gudmundsdóttir, *J. Am. Chem. Soc.* **2007**, *129*, 16263.
- [38] R. A. A. U. Ranaweera, J. Sankaranarayanan, L. Casey, B. S. Ault, A. D. Gudmundsdóttir, *J. Org. Chem.* **2011**, *76*, 8177.
- [39] S. Rajam, R. S. Murthy, A. V. Jadhav, Q. Li, C. Keller, C. Carra, T. C. S. Pace, C. Bohne, B. S. Ault, A. D. Gudmundsdóttir, *J. Org. Chem.* **2011**, *76*, 9934.
- [40] D. W. Gamage, Q. Li, R. A. A. U. Ranaweera, S. K. Sarkar, G. K. Weragoda, P. L. Carr, A. D. Gudmundsdóttir, *J. Org. Chem.* **2013**, *78*, 11349.
- [41] X. Zhang, S. K. Sarkar, G. K. Weragoda, S. Rajam, B. S. Ault, A. D. Gudmundsdóttir, *J. Org. Chem.* **2013**, *79*, 653.
- [42] R. F. Klima, A. V. Jadhav, P. N. D. Singh, M. Chang, C. Vanos, J. Sankaranarayanan, M. Vu, N. Ibrahim, E. Ross, S. McCloskey, R. S. Murthy, J. A. Krause, B. S. Ault, A. D. Gudmundsdóttir, *J. Org. Chem.* **2007**, *72*, 6372.
- [43] C. Phys. Rev. B: Condens. Matter Lee, W. Yang, R. G. Parr, *Phys. Rev. B Condens. Matter* **1988**, *37*, 785.
- [44] C. Gonzalez, H. B. Schlegel, *J. Chem. Phys.* **1989**, *90*, 2154.
- [45] C. Gonzalez, H. B. Schlegel, *J. Phys. Chem.* **1990**, *94*, 5523.
- [46] J. K. Labanowski, J. W. Andzelm, *Springer-Verlag*, New York, **1991**.
- [47] R. G. Parr, Y. Weitao, *Density Functional Theory in Atoms and Molecules*, Oxford University Press, Oxford, **1989**.
- [48] R. Bauernschmitt, R. Ahlrichs, *Chem. Phys. Lett.* **1996**, *256*, 454.
- [49] R. E. Stratmann, G. E. Scuseria, M. J. Frisch, *J. Chem. Phys.* **1998**, *109*, 8218.
- [50] J. B. Foresman, M. Head-Gordon, J. A. Pople, M. J. Frisch, *J. Phys. Chem.* **1992**, *96*, 135.
- [51] J. Tomasi, B. Mennucci, R. Cammi, *Chem. Rev.* **2005**, *105*, 2999.
- [52] B. Mennucci, E. Cancès, J. Tomasi, *J. Phys. Chem. B* **1997**, *101*, 10506.
- [53] E. Cancès, B. Mennucci, *J. Chem. Phys.* **2001**, *114*, 4744.
- [54] J. Tomasi, M. Persico, *Chem. Rev. (Washington, D. C.)* **1994**, *94*, 2027.
- [55] C. J. Cramer, D. G. Truhlar, *Chem. Rev. (Washington, D. C.)* **1999**, *99*, 2161.
- [56] S. Muthukrishnan, J. Sankaranarayanan, R. F. Klima, T. C. S. Pace, C. Bohne, A. D. Gudmundsdóttir, *Org. Lett.* **2009**, *11*, 2345.